

In Situ Formation Process of LiCoO_2 in the Molten Lithium-Potassium Carbonate Eutectic at 923 K

Kohta YAMADA and Isamu UCHIDA*

Department of Molecular Chemistry & Engineering, Faculty of Engineering,
Tohoku University, Aramaki-Aoba, Aoba-ku, Sendai 980

The spontaneous oxidation of Co metal in a molten (62Li+38K)mol% carbonate mixture with an oxygen partial pressure has been characterized at 923 K. When a thin Co film electroplated on a gold substrate was immersed into the melt, the open circuit potential (OCP) decayed gradually, indicating well-defined, three potential plateaus, and the oxide films produced at each potential plateau were identified by X-ray diffraction. The surface products at the first and second plateaus were $\text{Co}^{\text{II}}\text{O}$, but the film impedance decreased rapidly at the second plateau, suggesting the formation of the lithiated $\text{Co}^{\text{II}}\text{O}$. It was found that $\text{LiCo}^{\text{III}}\text{O}_2$ was formed at the third OCP plateau (ca. -0.4 V vs. (1:2) O_2/CO_2 reference electrode) and OCP reached to the Nernst potential of oxygen electrode reaction after the completion of LiCoO_2 formation.

In molten carbonate fuel cell (MCFC) technology, the dissolution of the state-of-the-art lithiated NiO cathode is one of the major life-limiting factors. An important approach to this problem is to develop an alternative cathode material. Recently, great attentions have been given to LiCoO_2 as the most promising cathode material. Its stability and electrochemical properties in molten alkali carbonates have been investigated by ECN group¹⁻⁴⁾ and other researchers.⁵⁻⁷⁾ The LiCoO_2 electrodes tested were fabricated by powder synthesis and sintering. In our laboratory, the in situ metal oxidation process in molten alkali carbonates have been investigated using electrochemical techniques.^{8,9)} In the present report, we have described the electrochemical behavior and in situ formation process of LiCoO_2 in (62+38)mol% (Li+K) CO_3 melt.

The apparatus and the experimental procedures were identical with those described in the previous work.⁹⁾ The working electrodes were fully immersed and consisted of a thin layer of cobalt ($1.0\text{ }\mu\text{m}$) electroplated on a gold flag of a geometric area equal to 0.39 cm^2 . Those electrodes will be further denoted as Co/Au in this article. The ac impedance plots at 1 kHz and the open circuit potential of the Co/Au electrodes during the LiCoO_2 formation were recorded simultaneously in (62+38)mol% (Li+K) CO_3 at 923 K under (9:1) O_2/CO_2 . The electrode potential was measured with respect to an oxygen gas reference electrode fed with (1:2) O_2/CO_2 . The surface analysis of electrode was carried out by a Shimadzu X-ray diffractometer XD-610 with the thin film attachment (with the incident angle equal to 8 degree).

The decay of the open circuit potential (OCP) and the film impedance of a Co($1\text{ }\mu\text{m}$)/Au electrode is shown in Fig.1. The OCP varied from around -0.88 V to the electrode potential predicted by the Nernst's

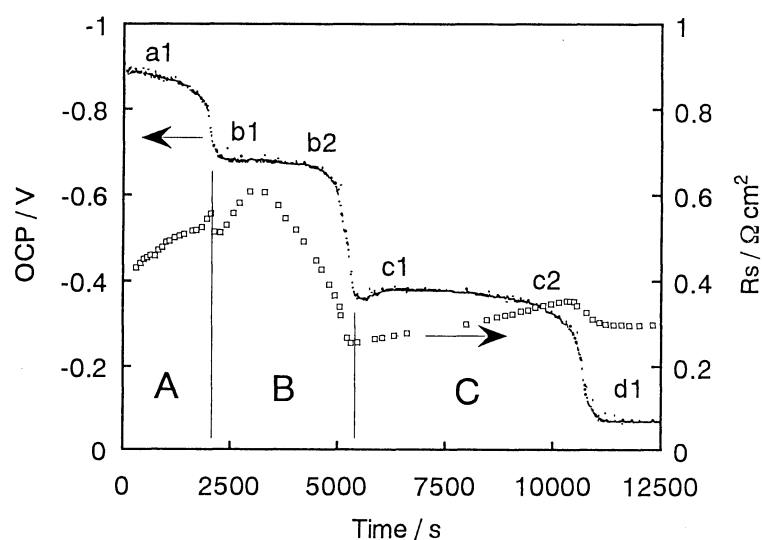


Fig. 1. Open circuit potential decay and impedance change during the open circuit oxidation for Co(1 μm)/Au in (62+38)mol%(Li+K)CO₃ at 923 K under O₂/CO₂=0.9/0.1 atm.

Table 1. Surface products of Co/Au electrodes determined from XRD analyses. The symbols, a1, b1, b2, c1, c2 and d1 indicate the sampling points in Fig. 1

Sampling point	Surface product
a1	CoO
b1	CoO
b2	CoO
c1	CoO + LiCoO ₂
c2	LiCoO ₂
d1	LiCoO ₂

equation for a gold electrode within a duration of over 3 h (11000 s). It should be noted that the OCP decay shows the three plateau regions (denoted as A,B,C in Fig.1). The surface of the electrode was also examined by the X-ray diffraction (XRD) method at the particular steps of the oxidation process. The surface products detected when the OCP decay approaches points a1, b1, b2, c1, c2 and d1 (in Fig.1) are reported in Table 1. The XRD pattern at d1 indicated LiCo^{III}O₂. It means that the overall process of the oxidation proceeds from Co(0) to Co(III). Moreover, the surface oxide layer undergoes also the incorporation of Li⁺ ion during the oxidation. Therefore, the presence of successive potential arrests in the OCP decay must be attributed to the change of oxidation state of cobalt and the diffusion of Li⁺ ion into the oxide layer. It is also known that the conductivity of cobalt oxide layer may change due to the incorporation of small amount of Li⁺ ions, as it is in the case of lithiated NiO cathode.¹⁰⁾ As shown in Fig. 1, the change of film impedance corresponded with the potential arrests. The impedance decreases rapidly when OCP passes the B region at the potential -0.68 V. Accordingly, it is reasonable to suppose that the lithiation process takes place in the plateau region. However, the XRD pattern of the surface product did not indicate the presence of lithiated CoO (Li-Co^{II}O). It is likely so,

because the amount of Li^+ ion in the oxide layer is lower than the sensitivity of the apparatus.

The OCP in the A region was around -0.88 V, which is near -0.871 V, the standard electrode potential of $\text{Co}^0/\text{Co}^{\text{II}}\text{O}$ calculated from thermodynamic data.¹¹⁾ The surface product was black and its XRD pattern indicated $\text{Co}^{\text{II}}\text{O}$. The film impedance increased gradually, indicating the growth of $\text{Co}^{\text{II}}\text{O}$ layer, which has a low electric conductivity. Therefore, the oxidation of Co^0 to $\text{Co}^{\text{II}}\text{O}$ takes place in this region. However, it is an unsettled question why the film impedance attains its maximum within the B region.

The plateau around -0.40 V involves the most sluggish oxidation process. The surface product in this C region is black. Its XRD pattern at c1 indicated $\text{Co}^{\text{II}}\text{O}$ with a small addition of $\text{LiCo}^{\text{III}}\text{O}_2$, and that at c2 $\text{LiCo}^{\text{III}}\text{O}_2$ alone. These results provide evidences that the oxidation of $\text{Co}(\text{II})$ to $\text{Co}(\text{III})$ occurs simultaneously with the diffusion of Li^+ ion into the $\text{Li-Co}^{\text{II}}\text{O}$ layer. Assuming that the conductance of $\text{LiCo}^{\text{III}}\text{O}_2$ is smaller than that of $\text{Li-Co}^{\text{II}}\text{O}$, we can explain the slight increase of the impedance in this region. The formation of $\text{LiCo}^{\text{III}}\text{O}_2$ begins at oxide layer/melt interface, then proceeds inward causing the growth of $\text{LiCo}^{\text{III}}\text{O}_2$ layer and consequently increasing its impedance. The behavior of the potential arrest seems to be similar to the potential arrest observed in chronopotentiometry, as it has been described for Ni/Au electrodes in the previous paper.⁹⁾ The same situation seems to occur in the case of Co/Au electrodes, i.e. when the oxidation of $\text{Co}(\text{0})$ to $\text{Co}(\text{II})$ or that of $\text{Co}(\text{II})$ to $\text{Co}(\text{III})$ during lithiation process or that of $\text{Co}(\text{II})$ to $\text{Co}(\text{III})$ is finished, the potential will change drastically.

After completion of the oxidation process, the OCP attains the equilibrium potential predicted by the Nernst's equation, and the $\text{LiCo}^{\text{III}}\text{O}_2$ electrode works well as a stable cathode for oxygen reduction. Fig.2 shows the cyclic voltammogram of oxygen reduction under $(9:1)\text{O}_2/\text{CO}_2$ at $\text{LiCo}^{\text{III}}\text{O}_2$ electrode, which was fabricated by in situ oxidation of $\text{Co}(0.1\mu\text{m})/\text{Au}$ electrode. The oxygen reduction current at first wave was observed around OCP. It is noteworthy that the second wave appeared at around -0.5 V. An explanation for the second wave may be that the redox reaction of $\text{Co}(\text{II})/\text{Co}(\text{III})$ takes place in the oxide layer. Further investigations including the stability and the electrochemical characterization in the melt are now in progress.

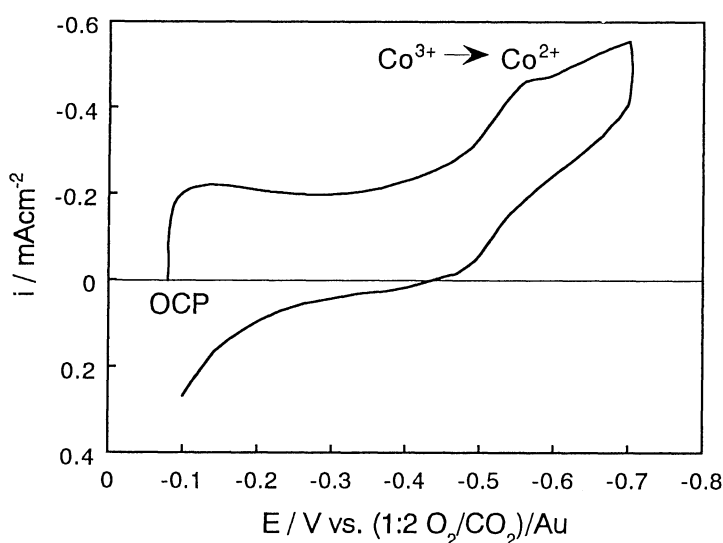


Fig. 2. Cyclic voltammograms of oxygen reduction on $\text{Co}(0.1\mu\text{m})/\text{Au}$ in $(62+38)\text{mol}\%(\text{Li}+\text{K})\text{CO}_3$ at 923 K under $\text{O}_2/\text{CO}_2=0.9/0.1$ atm. $v=0.2$ V/s.

The authors are particularly indebted to Dr. P. Tomczyk for his help in the preparation of this article and the many useful suggestions for its improvement.

References

- 1) L. Plomp, E. F. Sitters, J. P. P. Huijsmans, and S. B. van der Molen, "Molten Carbonate Fuel Cell Technology," ed by J. R. Selman, D. Shores, H. Maru, and I. Uchida, The Electrochemical Society Softbound Proceedings Series, Pennington, NJ (1990), PV **90-16**, p. 247.
- 2) L. Plomp, E. F. Sitters, C. Vessies, and F. C. Eckes, *J. Electrochem. Soc.*, **138**, 629 (1991).
- 3) J. B. J. Veldhuis, F. C. Eckes, and L. Plomp, *J. Electrochem. Soc.*, **139**, L6 (1992).
- 4) L. Plomp, E. F. Sitters, J. B. J. Veldhuis, R. C. Makkus, and S. B. van der Molen, "Carbonate Fuel Cell Technology," ed by D. Shores, H. Maru, I. Uchida, and J. R. Selman, The Electrochemical Society Softbound Proceedings Series, Pennington, NJ (1993), PV **93-3**, p. 171.
- 5) J. L. Smith, G. H. Kucera, and A. P. Brown, "Molten Carbonate Fuel Cell Technology," ed by J. R. Selman, D. Shores, H. Maru, and I. Uchida, The Electrochemical Society Softbound Proceedings Series, Pennington, NJ (1990), PV **90-16**, p. 226.
- 6) H. Koch, B. Rohland, and H. Wendt, 1992 Fuel Cell Seminar Abstracts, Arizona (1992), p. 277.
- 7) B. Bergman, C. Lagergren, and A. Lundblad, "Carbonate Fuel Cell Technology," ed by D. Shores, H. Maru, I. Uchida, and J. R. Selman, The Electrochemical Society Softbound Proceedings Series, Pennington, NJ (1993), PV **93-3**, p. 342.
- 8) I. Uchida, Y. Mugikura, T. Nishina, and K. Itaya, *J. Electroanal. Chem.*, **206**, 241 (1986).
- 9) T. Nishina, K. Takizawa, and I. Uchida, *J. Electroanal. Chem.*, **263**, 87 (1989).
- 10) J. R. Selman, and L. G. Marianowski, "Molten Salts Technology," ed by D. G. Lovering, Plenum Press New York and London (1982), p. 323.
- 11) J. R. Selman, and H. C. Maru, "Advances in Molten Salt Chemistry," Plenum Press New York and London (1981), Vol. 4, p. 159.

(Received November 1, 1993)